Journal of Applied Polymer Science

Electropreparation of (±)-10-Camphorsulfonate-Doped Poly(*o*-phenylenediamine) in Acetonitrile and Its Use in Determination of Glucose

Bülent Zeybek,[1,2] Nuran Özçiçek Pekmez,[3] Esma Kılıç[1]
[1]Department of Chemistry, Ankara University, 06100 Ankara, Turkey
[2]Department of Chemistry, Dumlupınar University, 43100 Kütahya, Turkey
[3]Department of Chemistry, Hacettepe University, 06800 Ankara, Turkey
Correspondence to: B. Zeybek (E - mail: bzeybek43@hotmail.com)

ABSTRACT: Poly(*o*-phenylenediamine) (P*o*PD) film has been electrochemically prepared on Pt electrode in an acetonitrile–water medium containing *o*-phenylenediamine (*o*PD) monomer and (±)-10-camphorsulfonic acid (HCSA) by using the cyclic voltammetry (CV). The P*o*PD film (P*o*PD–CSA) has been characterized by FTIR, CV, EIS, FESEM, and conductivity measurement. The glucose biosensor (Pt/P*o*PD–CSA/GOx) has been prepared from the P*o*PD coated electrode by immobilizing glucose oxidase (GOx) enzyme using glutaraldehyde. The biosensor shows a low detection limit and wide linear working range, a good reusability, long-term stability, and anti-interference ability. The Pt/P*o*PD–CSA/GOx has possesses higher sensitivity (2.05 μA/mmol L^{-1}) and affinity to glucose due to the use of CSA ion as dopant. The linear concentration ranges of Pt/P*o*PD–CSA/GOx have been found to be 9.6×10^{-3} to 8.2 mmol L^{-1} from calibration curve and 4.6×10^{-2} to 100 mmol L^{-1} from the relationship between the (1/glucose concentration) and (1/current difference). © 2013 Wiley Periodicals, Inc. J. Appl. Polym. Sci. **2014**, *131*, 39864.

KEYWORDS: conducting polymers; electrochemistry; sensors and actuators; poly(*o*-phenylenediamine); (±)-10-camphorsulfonic acid; glucose

Received 30 May 2013; accepted 17 August 2013
DOI: 10.1002/app.39864

INTRODUCTION

The fast and accurate determination of the glucose in blood for diagnosis of diabetes mellitus is very important. Ever since Clark and Lyons reported the first enzyme electrode for glucose determination, many studies have been performed to develop the enzyme-based glucose biosensors. The amperometric determination of glucose has been generally accomplished at a constant potential oxidation of hydrogen peroxide formed as a result of the reaction with glucose and glucose oxidase enzyme in the presence of oxygen.[1,2]

$$\beta\text{-D-glucose} + O_2 \xrightarrow{\text{GOx}} \text{D-gluconic acid} + H_2O_2 \quad (1)$$

$$H_2O_2 \rightarrow O_2 + 2H^+ + 2e^- \quad (2)$$

Nonconducting polymers have been used as a new support matrix for the immobilization of biomolecules. These polymer films display advantages such as permselectivity, which is useful in preventing the interfering of species in biological samples, fast response time and high reproducibility. Composite structures or materials including nonconducting polymers, like polyphenol and its derivatives, polyphenylenediamines and overoxidized polypyrrole could be used for amperometric biosensor design.[3,4] Poly(*o*-phenylenediamine) (P*o*PD) films have been especially used in the preparation of amperometric enzyme electrode for glucose determination.[3,5–9]

P*o*PD, one of the most studied derivatives of polyaniline, has attracted much interest in recent years. Many studies related to P*o*PD have been carried out with respects to the polymerization mechanism,[10–12] structure,[10–13] stability,[14] conductivity,[15–18] redox transformation,[13,19] and applications.[5,12,20–22] Chiba et al. suggested the structure of P*o*PD to be formed from the electropolymerization of *o*-phenylenediamine (*o*PD) in an acidic aqueous medium, which was a ladder polymer with phenazine rings.[10] According to the obtained IR absorption spectral data, the authors reported that the ladder polymer had a partially ring-opened structure, including parts of the oxidized forms of the quinine-imine type. Also, the three redox states of P*o*PD had reduced, semioxidized, and total-oxidized states. The semioxidized state was the most stable state and the major structure among them.[10,19] However, Yano proposed that the P*o*PD

Additional Supporting Information may be found in the online version of this article.

polymeric backbone had linear 1,4-substituted benzenoid–quinoid structure.[11] P*o*PD film has been synthesized electrochemically in aqueous media, such as H_2SO_4,[13] H_2SO_4 + Na_2SO_4,[10] H_3PO_4,[23] $HClO_4$ + $NaClO_4$,[24] acetate buffer,[5] and phosphate buffer.[7] Furthermore, the counter anions play a crucial role in the electrical, electrochemical, even optical properties of conducting polymers.[25] (±)-10-Camphorsulfonic acid (HCSA) is an organic acid with large size and it not only contributes to the protonation of monomer and/or polymeric species but also interacts with the conjugated chains of polymer through SO_3^- and C═O groups.[26] In literature, it was shown that the conducting polymer such as polyaniline,[27] poly(1-naphthylamine),[28] poly(3-methylpyrrole)[29] have been synthesized in the presence HCSA. There is no such study about the electrosynthesis of P*o*PD polymer in both aqueous and nonaqueous media containing HCSA.

In this paper, we report the electrochemical synthesis of (±)-10-camphorsulfonate (CSA^-) doped P*o*PD–CSA film on Pt electrode by cyclic voltammetry method in acetonitrile–water medium containing *o*PD and HCSA. It was compared with P*o*PD–ClO_4 film electrosynthesized in acetonitrile medium containing *o*PD and perchloric acid ($HClO_4$). The P*o*PD films were characterized by FTIR, conductivity measurement, CV, EIS, and FESEM. Then, glucose biosensors were prepared by immobilizing glucose oxidase enzyme using glutaraldehyde on the P*o*PD–CSA and P*o*PD–ClO_4 coated electrodes. The responses of these glucose biosensors were determined by the electrochemical oxidation of the enzymatically generated H_2O_2 at +0.7 V versus Ag/AgCl.

EXPERIMENTAL

Chemicals and Apparatus

The chemical reagents (±)-10-camphorsulfonic acid (Aldrich), *o*-phenylenediamine (1,2-diaminobenzene, Aldrich), glucose oxidase (GOx, from *Aspergillus niger*, 50,000 Unit Type II Sigma), glutaraldehyde (grade II, Sigma), silver nitrate ($AgNO_3$, Fluka), acetonitrile (Riedel de Haën, HPLC grade), *di*-sodium monohydrogen phosphate heptahydrate, sodium dihydrogen phosphate dihydrate (Riedel de Haën), hydrogen peroxide (H_2O_2, 35%, Riedel de Haën), D-(+)-glucose anhydrous (Fluka), tetrabutylammonium perchlorate (TBAP, Fluka), perchloric acid ($HClO_4$, Merck) were analytical grade and used without any further purification. Hydrogen peroxide and glucose solutions were prepared with 0.15 mol L^{-1} phosphate buffer solution (PBS, pH 7.0). Glucose stock solutions were allowed to mutarotate at room temperature overnight before use. All aqueous solutions were prepared with ultrapure water (18.2 MΩ cm) obtained from Elga Purelab (Veolia Water Systems, UK) device. All of the experiments were performed at room temperature.

Electrochemical measurements were performed in a single compartment three-electrode cell stand (BAS C3 cell stand, USA). The cylinder rod of platinum (Pt) disc with 4-mm diameter (0.1256 cm^2) was embedded into a 6-mm diameter polyetheretherketone (PEEK) cylinder holder to prepare working electrodes. Platinum foil with 1 cm^2 surface areas as the counter electrode and a silver wire in contact with 0.01 mol L^{-1} $AgNO_3$ as the reference electrode were used in electropolymerization studies. The 0.01 mol L^{-1} $AgNO_3$ in the reference electrode was dissolved in acetonitrile containing 0.1 mol L^{-1} TBAP as the supporting electrolyte. Platinum wire (BAS MW-1032) as counter electrode and Ag/AgCl (BAS MF-2052 RE-5B) as the reference electrode were used in amperometric studies. Before each experiment, the surface of Pt electrode was polished by using polishing kit (BAS MF-2060) with 0.05 μm alumina slurry and 1 μm diamond polish. The Pt electrode was washed with ultrapure water after polishing and then immersed for 3 min in ethanol solution in ultrasonic bath. Ultimately, it was dried at room temperature. The solution containing monomer and electrolyte was purged with nitrogen gas for 10 min to remove the oxygen before electropolymerization. The P*o*PD films were first washed several times with acetonitrile to remove adsorbed electrolyte, monomer and the soluble oligomers formed during electrosynthesis of the film, and then they were dried at room temperature.

Electrochemical studies were carried out using Ivium CompactStat (Ivium Technologies B.V, The Netherlands) electrochemical analyzer. Electrochemical behavior of P*o*PD films with and without GOx was examined in 1.0 mol L^{-1} KCl solution containing 5 mmol L^{-1} $Fe(CN)_6^{3-/4-}$ by CV and EIS. The cyclic voltammograms (CVs) were recorded in potential range between −0.2 and 0.6 V. The EIS measurements were performed at the frequency range between 10^5 and 10^{-2} Hz with 5 mV perturbation at open circuit potential (E_{OCP}). Fourier-transform infrared (FTIR) spectra of polymer films were directly recorded with Shimadzu IRaffinity-1 spectrometer with ATR attachment (Shimadzu Corporation, Japan). Scanning electron micrographs of polymer films with and without GOx were taken with a Jeol JSM-7000F Field Emission Scanning Electron Microscopy (FESEM) (Jeol, Japan). The dry conductivity of P*o*PD films were measured using the four-probe measuring technique at room temperature.

H_2O_2 Sensitivity Measurement of Pt/P*o*PD Electrodes

The Pt or Pt/P*o*PD electrode was placed in a cell containing 5 mL of 0.15 mol L^{-1} PBS (pH 7.0) and the solution was purged with nitrogen gas for 10 min. A constant potential of +0.7 V versus Ag/AgCl was applied and the background current was allowed to be constant. A certain volume from 1.0×10^{-2} mol L^{-1} H_2O_2 was injected into the cell. The steady-state current response to the addition of H_2O_2 was recorded and the current difference (Δi) was determined with the change between the steady-state current and the background current. Then, the relationship between Δi and H_2O_2 concentration was plotted.

Immobilization of GOx to Pt/P*o*PD Electrodes

Firstly, 100 U GOx was dissolved in 0.25 mL PBS (0.15 mol L^{-1}, pH 7.0) in an eppendorf tube and then 10 μL of 25% glutaraldehyde was added into enzyme solution. Afterward, the Pt/P*o*PD electrode was immersed vertically into enzyme solution including glutaraldehyde and then left overnight at +4°C in a refrigerator. The enzyme immobilized electrodes were denoted as Pt/P*o*PD–CSA/GOx and Pt/P*o*PD–ClO_4/GOx. Before each experiment, these electrodes were washed several times in

ultrapure water to remove nonimmobilized enzyme on the electrode surfaces.

Glucose Sensitivity Measurement of Pt/PoPD/GOx Electrodes

The Pt/PoPD–CSA/GOx electrode or Pt/PoPD–ClO_4/GOx electrode was placed in a cell containing 5 mL of 0.15 mol L^{-1} PBS (pH 7.0). A constant potential of +0.7 V versus Ag/AgCl was applied and the background current was allowed to be constant. The solution was continuously stirred with a magnetic stirrer at a rate of 300 rpm. D-(+)-glucose solution with certain concentration was injected into the cell after the solution purged with oxygen gas for about 60 s. The steady-state current response to the addition of glucose was recorded and the current difference (Δi) was determined with the change between the steady-state current and the background current. Then calibration curve of Δi–glucose concentration was plotted.

Michaelis–Menten kinetics, K_m and i_{max}, were obtained with Origin Pro 8 SR0 (evaluation edition) software by the use of calibration curve data of Pt/PoPD–CSA/GOx and Pt/PoPD–ClO_4/GOx electrodes. The kinetic values were calculated by using nonlinear curve fitting analysis Hill function [eq. (3)] in this software.[7]

$$i = i_{max} \frac{[glucose]}{K_m + [glucose]} \quad (3)$$

RESULTS AND DISCUSSION

Electrosynthesis of PoPD Polymers

To prepare (±)-10-camphorsulfonate (CSA^-) doped poly(*o*-phenylenediamine) (PoPD–CSA) film, the electropolymerization was performed in an acetonitrile solution containing *o*PD monomer and HCSA without using any electrolyte. But the white colored *o*-phenylenediaminium camphorsulfonate salt which was formed in this medium was not dissolved adequately. For this reason, the use of an acetonitrile–water mixture was planned as solvent and the range of 2–10% (v/v) water was added to acetonitrile. As the amount of water increased, the solubility of salt gradually increased and finally it totally dissolved at 7% water ratio. PoPD–CSA polymers were electrosynthesized between −0.4 and 2.2 V with 50 cycles on Pt electrode in these acetonitrile-water solutions, including 0.1 mol L^{-1} *o*PD and 0.2 mol L^{-1} HCSA. When the first cycles of these voltammograms were compared, it was observed that the oxidation peak potential of the protonated *o*PD monomer gradually shifted to 1.8 V from 1.4 V up to 6% water ratio, and then again decreased to about 1.4 V in the solution of 10% water. Also, the intensity of this peak increased up to 6% water ratio, and then it remained almost stationary. Besides, the most regular decrease in the oxidation peak intensities was determined at 6% water ratio when compared the successive cycles. Figure 1 shows the cyclic voltammogram recorded during electrosynthesis of PoPD–CSA in 94% acetonitrile-6% water medium including 0.1 mol L^{-1} *o*PD and 0.2 mol L^{-1} HCSA. In the first scan, the anodic current starts to increase at about 0.15 V and reaches to maximum value at 1.8 V, which corresponds to the oxidation of protonated *o*PD monomer. This irreversible peak shifts to negative potential and its intensity gradually decreases during the subsequent scans. The reduction waves appear at more negative potentials than 0.0 V in the reverse scans. These differences observed for each cycle could indicate the growth of the polymer. Indeed, it was observed that a brown–black colored film formed on the electrode surface at the end of 50 cycles scanning.

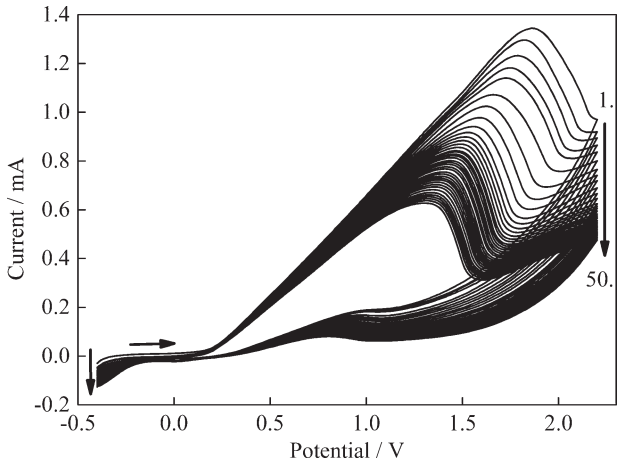

Figure 1. CVs recorded during the electrosynthesis of PoPD–CSA between –0.4 V and 2.2 V with 50 cycles on Pt electrode in 94% acetonitrile-6% water medium containing 0.1 mol L^{-1} *o*PD, and 0.2 mol L^{-1} HCSA, v = 25 mV s^{-1}.

The formation of the polymer can be summarized as follows. The protonated *o*PD monomer is oxidized at the positive potentials from 0.15 V in this medium forming its cation radical, then these radicals couple to form dimer as in the case of electropolymerization of aniline. The dimer cation radical reacts with the monomer cation radical, which is also formed at the potentials of monomer oxidation. Continuation of the same type reactions results in the formation of the oligomers and eventually the polymer.[30,31]

The effect of water content in acetonitrile on the amount of PoPD–CSA film deposited on Pt electrode was investigated. The total charge quantity which passed between 2nd and 50th cycles during electropolymerization versus the amount of water % in

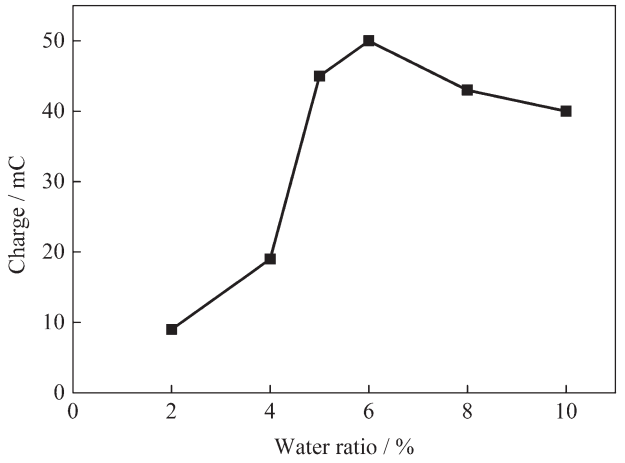

Figure 2. Plot of the total charge quantity passed between 2nd and 50th cycles during the electrosynthesis of PoPD–CSA versus the water ratio % in acetonitrile.

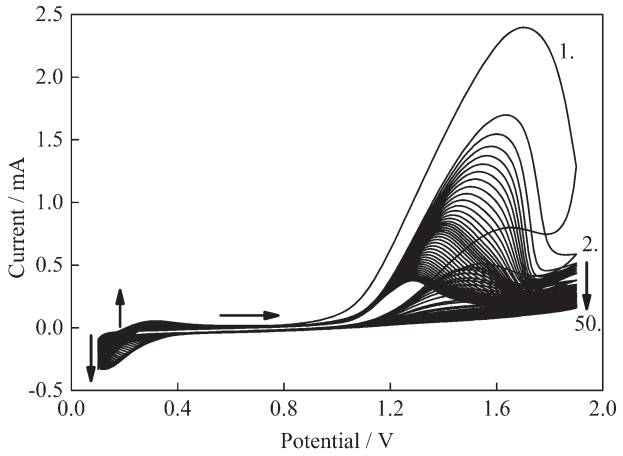

Figure 3. CVs recorded during the electrosynthesis of P*o*PD–ClO_4 between 0.1 V and 1.9 V with 50 cycles on Pt electrode in the acetonitrile solution containing 0.1 mol L^{-1} *o*PD and 0.2 mol L^{-1} $HClO_4$, $\nu = 25$ mV s^{-1}.

solution was plotted and given in Figure 2. It is known that the amount of film deposited on the electrode surface can be presumed to be proportional to the charge that passed during electropolymerization.[30,32] As seen in Figure 2, the rise in the yield of polymer is proportional to water concentration up to a maximum value around 6%. This could be a result of increased solubility of the monomer. After this point, the excess of water limits the amount of the polymer formed. This might be due to the increasing solubility of the CSA^- doped oligomeric species. It is determined that the most suitable solvent is 94% acetonitrile and 6% water mixture for the formation of P*o*PD–CSA polymer. This result shows that the water content of polymerization solution is an important parameter during the electropolymerization of protonated *o*PD monomer on the Pt electrode surface.

For comparison, perchlorate doped poly(*o*-phenylenediamine) (P*o*PD–ClO_4) film was electrosynthesized on Pt electrode in acetonitrile solution containing 0.1 mol L^{-1} *o*PD and 0.2 mol L^{-1} $HClO_4$. Figure 3 shows the cyclic voltammogram recorded during electrosynthesis of this film. The oxidation of protonated *o*PD monomer starts at about 0.9 V and reaches the maximum value at 1.7 V in the first cycle. As the cycle number increases, the oxidation peak potential shifts to negative potentials and its current intensity decreases in each successive cycle as in the case of P*o*PD–CSA. After the first scan, the intensities of the broad peaks at about 0.3 and 0.25 V due to the oxidation and reduction of the P*o*PD–ClO_4 film increase and shift to more anodic and cathodic values as the film grows, respectively. The oxidation peak of this film is observed in contrast to the case in P*o*PD–CSA polymer. In other words, the oxidation and reduction peaks of the P*o*PD–ClO_4 film are more reversible than that of other polymer. This could indicate the resistivity of P*o*PD–CSA film. As a result, a thin film with orange–brown color was observed on the electrode surface after 50 cycles scanning.

To determine the optimal molar ratio of monomer to acid, the P*o*PD films were formed from solutions including the fixed concentration of acid (0.2 mol L^{-1} HCSA or $HClO_4$) and the varying concentration of *o*PD (0.025−0.2 mol L^{-1}). The charge quantities that passed between 2nd and 50th cycles during the formation of P*o*PD–CSA and P*o*PD–ClO_4 polymers versus monomer concentration were plotted (Supporting Information Figure S1). The optimum monomer concentrations were 0.1 mol L^{-1} for P*o*PD–CSA film and between 0.1 and 0.125 mol L^{-1} for P*o*PD–ClO_4 film. In this medium, the concentration ratio of monomer to acid is about 1:2; in other words, both amine centers in *o*PD monomer might be protonated within the equilibrium state. The existence of sufficient amounts of protonated monomer in the electrode region provides the necessary condition for the stability of the cation radicals.[30] It can be concluded that monomer, dimer and oligomer cation radicals are stable under this condition for the growth of polymer chain.

Characterization of P*o*PD Polymers

FTIR Spectra. Figure 4(a,b) shows the FTIR spectra of P*o*PD–CSA and P*o*PD–ClO_4 films on Pt electrode, respectively. In the spectrum of P*o*PD–CSA film, the bands at 3368 and 3196 cm^{-1} are due to the N–H stretching vibrations of the —NH_2 and —NH groups in polymer chain.[10,33,34] The band observed at 1626 cm^{-1} can be assigned to the C=N stretching vibrations in phenazine ring.[10,24,34,35] The band located at 1530 cm^{-1} can be attributed to the C=C stretching vibrations in phenazine ring.[34,35] The band at 1373 cm^{-1} is related to the C—N stretching vibrations in quinoid rings.[10,21,23,24,34] The band at 1227 cm^{-1} corresponds to the C—N stretching vibrations in benzenoid rings.[21,23,34] The C—H in-plane bending vibration of the substituent benzene rings is observed at 1150 cm^{-1},[33,36] while the C—H out-of-plane bending vibrations of the substituent benzene rings are observed at 854 cm^{-1} and 758 cm^{-1}.[10,21,34,35] The bands at around 2957 cm^{-1} and 2887 cm^{-1} can be assigned to both C—H stretching vibrations in aromatic rings and C—H stretching vibrations of the CH_2 and CH_3 groups of CSA^-, respectively.[35,37] In addition, the bands at nearly 1734 cm^{-1} and 1036 cm^{-1} are assigned to the C=O and the S=O groups, respectively.[37] These bands indicate the presence of CSA^- as dopant ion in the structure of polymer.

In Figure 4(b), the main bands of the P*o*PD–ClO_4 polymer backbone are nearly similar to that of the P*o*PD–CSA. The stretching vibrations of the ClO_4^- anion are observed at

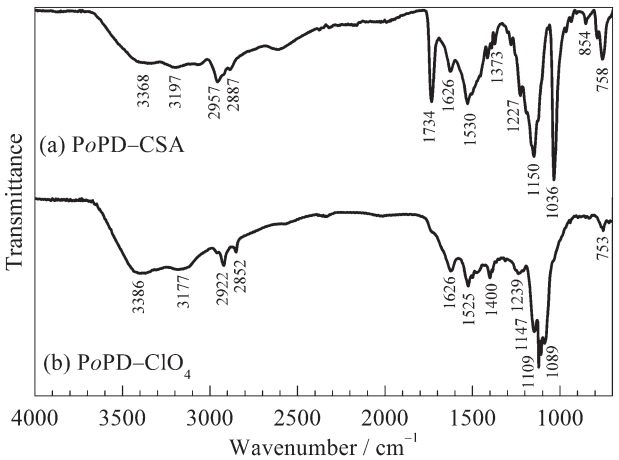

Figure 4. FTIR spectra of (a) PoPD–CSA and (b) P*o*PD–ClO_4 films.

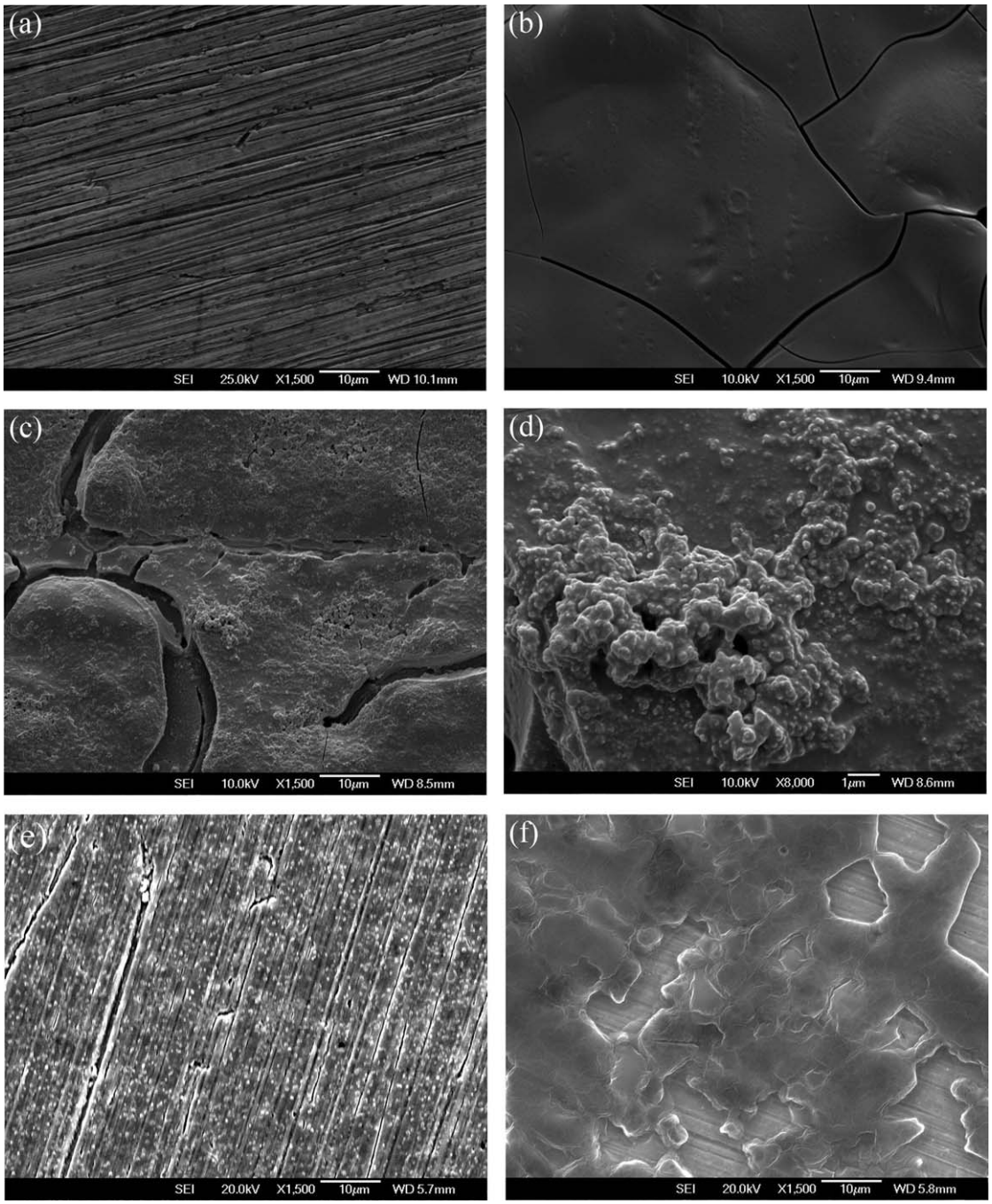

Figure 5. FESEM micrographs of (a) Pt, (b) Pt/PoPD–CSA, (c) Pt/PoPD–CSA/GOx, (d) Pt/PoPD–CSA/GOx, (e) Pt/PoPD–ClO_4, and (f) Pt/PoPD–ClO_4/GOx electrodes (while the image of (d) was magnified 8000 times, the other images were magnified 1500 times).

1109 cm^{-1} and 1089 cm^{-1}.[24] The ratio of the peak intensity of the C═N and C═C vibrations to the S═O vibration for PoPD–CSA are bigger than the ratio of the C═N and C═C vibrations to the ClO_4^- vibration for PoPD–ClO_4. In other words, the amount of dopant anion in the PoPD–CSA film is less than that of the PoPD–ClO_4 film. This result shows that the ladder structure is dominant species in PoPD–CSA film.

Dry Conductivities. The dry conductivity values of polymer films were measured using the four-probe measuring technique. The conductivity values of PoPD–CSA and PoPD–ClO_4 films were about 2.0×10^{-6} S cm^{-1} and 1.0×10^{-5} S cm^{-1}, respectively. The poor conductivities could be due to the deficiency of charge carriers on PoPD polymer backbone or due to the low mobility of carriers.[38] In some previous studies, the conductivity values of PoPD films synthesized in aqueous medium were reported to be 4.3×10^{-10} S cm^{-1} [16], 2.23×10^{-7} S cm^{-1} [39] in the presence of hydrochloric acid and 4.0×10^{-7} S cm^{-1} [18], 2.9×10^{-2} S cm^{-1} [15] in the presence of sulfuric acid, respectively. In this study, the dry conductivity value of PoPD–CSA is

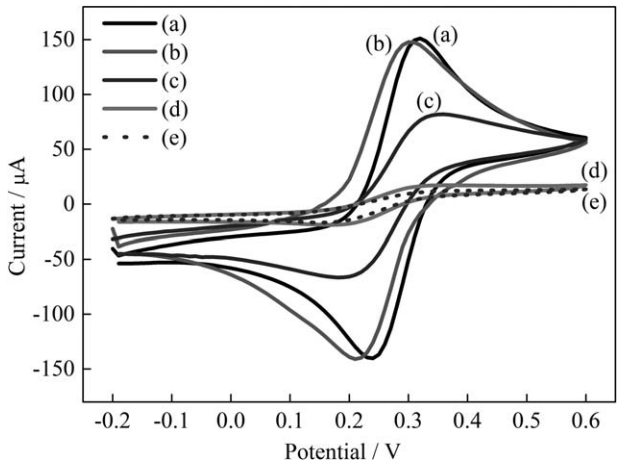

Figure 6. CVs of (a) Pt, (b) Pt/P*o*PD–CSA, (c) Pt/P*o*PD–ClO_4, (d) Pt/P*o*PD–CSA/GOx, and (e) Pt/P*o*PD–ClO_4/GOx electrodes recorded in 1.0 mol L^{-1} KCl solution containing 5 mmol L^{-1} $Fe(CN)_6^{3-/4-}$, ν = 50 mV s^{-1}.

five times less than that of P*o*PD–ClO_4, which is due to the decreasing conjugation length of polymer chains or the size effect on mobility of counter anion (CSA^-) in polymer.[38]

FESEM Micrographs. Figure 5 shows FESEM micrographs of bare Pt, Pt/P*o*PD–CSA, Pt/P*o*PD–ClO_4, Pt/P*o*PD–CSA/GOx, and Pt/P*o*PD–ClO_4/GOx electrodes. Pt/P*o*PD–ClO_4 exhibits rough structures. On the other hand, P*o*PD–CSA film exhibits smooth structures with cracks between them. These cracks can result from the ladder structure of P*o*PD–CSA, which is dominant species in the polymer.[21,40,41] As seen in Figure 5, the surface images of GOx immobilized P*o*PD films are different from those of P*o*PD films. While the globular particles have been observed on the surface of Pt/P*o*PD–CSA/GOx electrode, a more compact structure has been observed on the surface of Pt/P*o*PD–ClO_4/GOx electrode. Consequently, it can be concluded that GOx enzyme is immobilized on the surface of P*o*PD films.

Electrochemical Behaviors. The electron transfer of ferro-ferricyanide ion ($Fe(CN)_6^{3-/4-}$) through the modified electrode could be used as a useful tool to monitor the electrode construction process.[42] The effect of P*o*PD–CSA and P*o*PD–ClO_4 films with and without GOx on electron transfer features of Pt electrode was investigated in 1.0 mol L^{-1} KCl solution containing 5 mmol L^{-1} $Fe(CN)_6^{3-/4-}$. Figure 6 shows the cyclic voltammograms of $Fe(CN)_6^{3-/4-}$, obtained on bare and polymer coated Pt electrodes. A well-defined redox peak is observed for bare Pt and Pt/P*o*PD–CSA on the contrary to the other electrodes. In the case of P*o*PD–ClO_4, the peak currents considerably decrease on the P*o*PD–ClO_4 electrode when compared to that of Pt electrode. While the peak-to-peak separation of $Fe(CN)_6^{3-/4-}$ waves ($E_{p,a} - E_{p,c} = \Delta E_p$) is 60 mV for the Pt electrode, the ΔE_p are 80 and 160 mV for the Pt/P*o*PD–CSA and Pt/P*o*PD–ClO_4 electrodes, respectively. These observations indicate that oxidation and reduction of $Fe(CN)_6^{3-/4-}$ predominantly occurs on Pt surface instead of polymer coating due to the cracks especially for the Pt/P*o*PD–CSA. However, the peak currents significantly decrease at Pt/P*o*PD–CSA/GOx, and Pt/P*o*PD–ClO_4/GOx electrodes as seen in Figure 6, which are considerably block oxidation and reduction reactions of the $Fe(CN)_6^{3-/4-}$ redox probe.[43,44] This means that the P*o*PD–CSA and P*o*PD–ClO_4 films and their cracks are covered with GOx enzyme after immobilization.

EIS Spectra. Electrochemical impedance spectrum (EIS) is an effective method to investigate the electrical properties of modified electrodes and for understanding electrochemical reaction rates. In a typical impedance spectrum, Nyquist curve consists of a semicircle part at high frequencies and a linear part at low frequencies. The semicircle part and the linear part correspond to the electron transfer limited process and the diffusion limited process, respectively. The diameter of the semicircle equals to electron transfer resistance (R_{et}).[45] Figure 7 shows the EIS of P*o*PD coatings with and without GOx and also bare Pt electrode. The Nyquist impedance plots of bare Pt and Pt/P*o*PD–CSA electrodes present nearly a straight line at all frequencies. The R_{et} values of the Pt and Pt/P*o*PD–CSA electrodes are very small. The resemblances of EIS spectra confirm the presence of the cracks in the resulting P*o*PD–CSA polymer. The Nyquist impedance curves of Pt/P*o*PD–ClO_4, Pt/P*o*PD–CSA/GOx, and

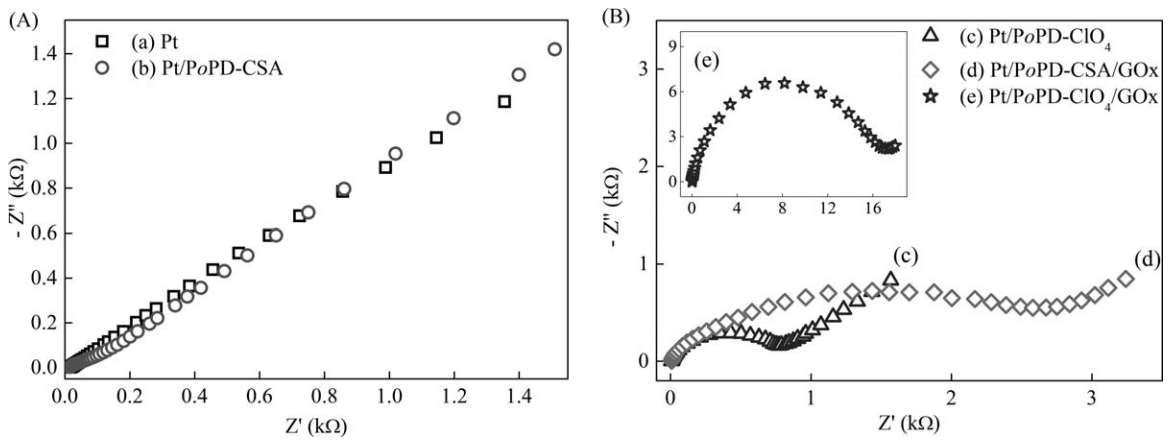

Figure 7. (A) Nyquist plots of (a) Pt, (b) Pt/P*o*PD–CSA, (B) (c) Pt/P*o*PD–ClO_4, (d) Pt/P*o*PD–CSA/GOx, and (e) Pt/P*o*PD–ClO_4/GOx electrodes recorded in 1.0 mol L^{-1} KCl solution containing 5.0 mmol L^{-1} $Fe(CN)_6^{3-/4-}$

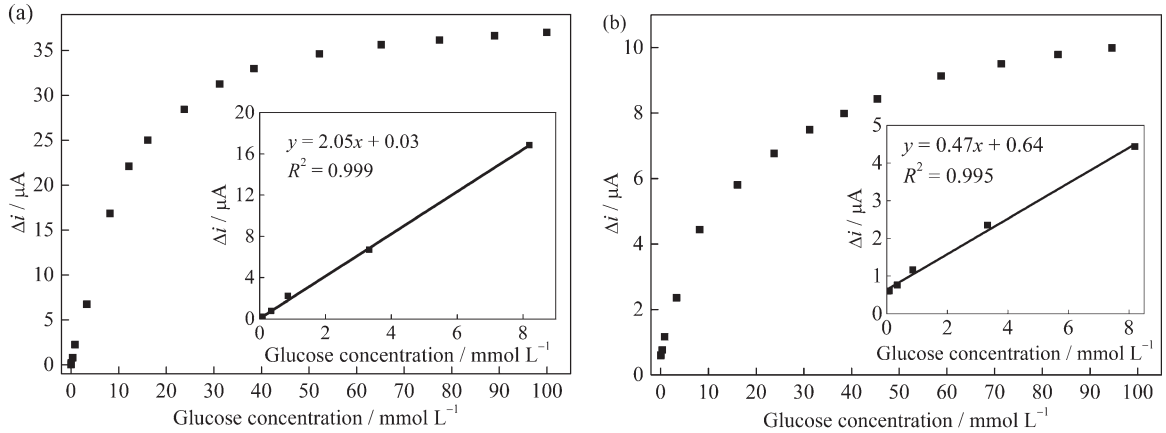

Figure 8. Calibration curves of glucose obtained at +0.7 V versus Ag/AgCl for (a) Pt/PoPD–CSA/GOx and (b) Pt/PoPD–ClO_4/GOx electrodes (0.15 mol L^{-1} PBS, pH 7.0).

Pt/PoPD–ClO_4/GOx electrodes exhibit a depressed semicircle at high frequencies and a straight line at low frequencies (Figure 7) and their R_{et} values are about 740, 2940, and 16,700 ohm, respectively. As a result, the R_{et} values significantly increase, when the GOx enzyme is immobilized on the polymer-coated electrode surface. It is suggested that GOx layer behaves as an obstacle to electron transfer at the electrode surface. Furthermore, the electron transfer property of Pt/PoPD–CSA/GOx is higher than that of Pt/PoPD–ClO_4/GOx due to the CSA^- as dopant when compared to their R_{et} values.

Determination of Glucose

H_2O_2 Sensitivity of Pt and Pt/PoPD Electrodes. Supporting Information Figure S2 illustrates the relationship between the current difference values and H_2O_2 concentration at +0.7 V versus Ag/AgCl for Pt, Pt/PoPD–CSA, and Pt/PoPD–ClO_4 electrodes. The slopes of curves are quite similar to each other when compared. While the PoPD film selectively allows the permeation of H_2O_2, which is a small molecule, it limits the access of large molecules to the electrode surface.[5,6] It can be concluded that the PoPD coated electrodes can be used to develop enzyme electrodes based on the oxidation of H_2O_2 formed from the reaction between substrate and enzyme.

Glucose Sensitivity of Pt/PoPD/GOx Electrodes. The Pt/PoPD–CSA/GOx and Pt/PoPD–ClO_4/GOx electrodes were prepared from the PoPD coated electrodes by immobilizing GOx enzyme using glutaraldehyde. The responses of these electrodes toward glucose were determined via monitoring the current corresponding to the oxidation of the enzymatically produced H_2O_2 at +0.7 V versus Ag/AgCl. The calibration curves for glucose obtained for Pt/PoPD–CSA/GOx and Pt/PoPD–ClO_4/GOx electrodes are shown in Figure 8. The linear concentration ranges of Pt/PoPD–CSA/GOx and Pt/PoPD–ClO_4/GOx electrodes were determined to be 9.6×10^{-3} to 8.2 mmol L^{-1} and 4.6×10^{-2} to 8.2 mmol L^{-1}, respectively. Forzani et al. have reported that the normal clinical range for glucose in blood is between 3.5 and 6.1 mmol L^{-1}.[46] The performance properties of some amperometric glucose biosensors based on PoPD reported in literature are given in Table I to be compared with the results of our study. The Pt/PoPD–CSA/GOx and Pt/PoPD–ClO_4/GOx electrodes can be used for the determination of glucose when compared the sensitivity and linear range of the enzyme electrodes in literature. In addition, it is desired to obtain the highest i_{max} and lowest K_m for construction of enzyme electrodes.[51] The K_m and i_{max} were determined to be 11.90 mmol L^{-1} and 42.17 μA for Pt/PoPD–CSA/GOx electrode and 14.26 mmol L^{-1} and 11.26 μA for Pt/PoPD–ClO_4/GOx electrode by using nonlinear curve fitting analysis, respectively. The obtained K_m values are smaller than those reported for glucose biosensors that include 14.2 mmol L^{-1} for Pt/PoPD/GOx,[5] 25.04 mmol L^{-1} for RVC/Pt/PoPD/GOx,[6] 29 ± 4 mmol L^{-1} for Pt/PoPD/GOx,[7] 22.0 ± 2.0 mmol L^{-1} for Pt/PoPD/GOx[8] electrodes, and 22.71 mmol L^{-1} for Pt/PPy–GOx/PoPD electrode.[3] This result shows that the Pt/PoPD–CSA/GOx and Pt/PoPD–ClO_4/GOx enzyme electrodes possess a higher affinity to glucose than that of the aforementioned biosensors.

The limit of detection (LOD) of the Pt/PoPD–CSA/GOx and Pt/PoPD–ClO_4/GOx electrodes were determined to be 6.5×10^{-5} mmol L^{-1} and 3.0×10^{-4} mmol L^{-1} ($S/N = 3$), respectively. LOD values are calculated according to following equation:

$$\mathrm{LOD} = \frac{3s}{m}$$

where s is the standard deviation of the background current (three runs), m is the slope of the related calibration curve. It can be concluded that the performance characteristics of these electrodes can compete with electrodes previously reported in the literature.

If the enzyme electrodes prepared in this study are compared, it can be seen that the Pt/PoPD–CSA/GOx enzyme electrode shows a higher linear concentration range and sensitivity (Table I). This can be due to three reasons. One of them is that the ratio of the ladder to benzenoid structures in PoPD–CSA polymer should be different from that in the PoPD–ClO_4 polymer. The ladder structure are the dominant species in the PoPD–CSA film prepared with the large sized CSA^- dopant when considered the colors of the resulted film and the conductivity values and the FTIR results mentioned above. Secondly, the electron transfer property of Pt/PoPD–CSA/GOx is better than that of Pt/PoPD–ClO_4/GOx according to EIS results.

Table I. Comparison of Performance Properties of Some Amperometric Glucose Biosensors Based on PoPD Reported in Literature[a]

Electrode	Applied potential	Linear range (mmol L^{-1})	Sensitivity (μA (mmol L^{-1})$^{-1}$)	K_m (mmol L^{-1})	i_{max} (or j_{max})	References
Pt/PoPD/GOx	0.7 V vs. SCE	-	-	14.2	12.8 μA	5
RVC/Pt/PoPD/GOx	0.6 V vs. SCE	-	-	25.04	46.60 μA	6
Pt/PoPD/GOx	0.7 V vs. SCE	-	-	29 ± 3	44 ± 8 nA	7
Pt/PoPD/GOx	0.7 V vs. SCE	Up to 7.0	-	22 ± 2	69.0 ± 12.6 μA cm^{-2}	8
Pt/PoPD/GOx	0.7 V vs. Ag/AgCl	Up to 10	-	-	-	47
Pt/PoPD/SiO_2-GOx	0.6 V vs. Ag/AgCl	2×10^{-3} to 2.0	0.82	4.3	1.2 μA	48
Pt/PPy−GOx/PoPD	0.7 V vs. Ag/AgCl	-	0.019	22.71	0.50 μA	3
GC/Cu/Pd/PoPD/GOx	0.7 V vs. Ag/AgCl	Up to 6.0	7.3	0.25	-	49
Pt/Pt/PoPD/GOx	0.7 V vs. Ag/AgCl	0.3–25	192 ±48 (μA cm^{-2} (mol L^{-1})$^{-1}$)	-	-	9
GC/Pt/PoPD-GOx	0.65 V vs. Ag/AgCl	0.0–5.0	0.99	-	-	50
Pt/PoPD/GOx (CSA)	0.7 V vs. Ag/AgCl	9.6×10^{-3} to 8.2	2.05	11.90	42.17 μA	This work
Pt/PoPD/GOx (ClO_4)	0.7 V vs. Ag/AgCl	4.6×10^{-2} to 8.2	0.47	14.26	11.26 μA	This work
Pt/PoPD/GOx (CSA)	0.7 V vs. Ag/AgCl	4.6×10^{-2} to 100	From Lineweaver-Burk curve (the second method)			This work
Pt/PoPD/GOx (ClO_4)	0.7 V vs. Ag/AgCl	3.3–94	From Lineweaver-Burk curve (the second method)			This work

[a] In literatures, some properties of biosensors were not reported.

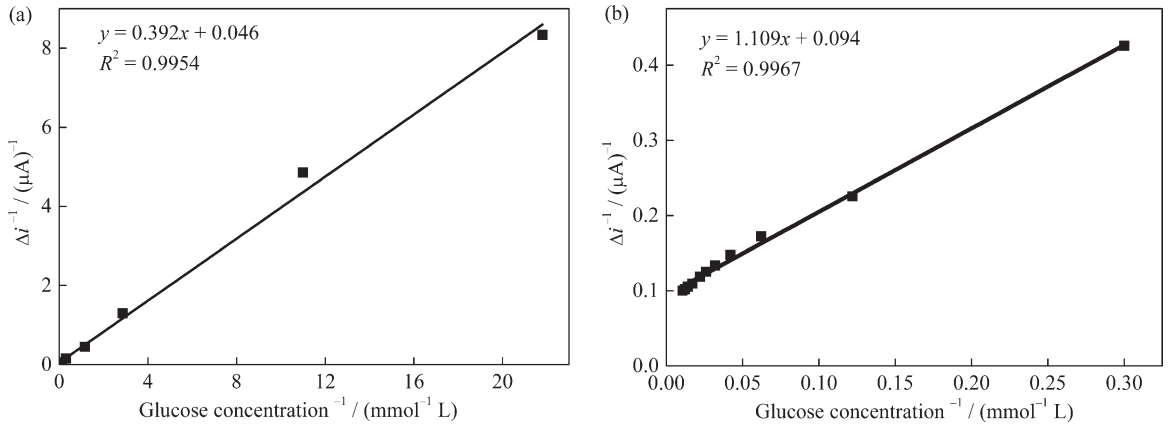

Figure 9. Relationship between the (1/glucose concentration) and (1/current difference) (Lineweaver–Burk curves) at +0.7 V versus Ag/AgCl for (a) Pt/P*o*PD–CSA/GOx and (b) Pt/P*o*PD–ClO_4/GOx electrodes (0.15 mol L^{-1} PBS, pH 7.0).

Thirdly, the covalent bonding between P*o*PD–CSA polymer and GOx enzyme may be stronger than that of P*o*PD–ClO_4 polymer in PBS.[52]

In this study, the relationship between the (1/glucose concentration) and (1/current difference) (Lineweaver–Burk curves) was also plotted as the second method to determine of the linear concentration ranges of biosensors. The graphics for Pt/P*o*PD–CSA/GOx and Pt/P*o*PD–ClO_4/GOx electrodes are shown in Figure 9. The linear working ranges of Pt/P*o*PD–CSA/GOx and Pt/P*o*PD–ClO_4/GOx electrodes were determined to be 4.6×10^{-2} to 100 mmol L^{-1} (R^2 = 0.996) and 3.3−94 mmol L^{-1} (R^2 = 0.997), respectively. The upper value of the linear concentration ranges is higher than that of the first method (calibration curves). As a result, extremely high concentration of glucose can be determined by the second method.

Interference Studies. The presence of interferences, such as ascorbic acid (AA), uric acid (UA), and urea (U), in the biological sample can block the signal of glucose. The physiological level of glucose is about 50 times higher than that of interfering species.[53] In this study, the performance of the (a) Pt/P*o*PD–CSA/GOx and (b) Pt/P*o*PD–ClO_4/GOx electrodes was evaluated in the presence of 0.1 mmol L^{-1} AA, 0.1 mmol L^{-1} UA, and 0.8 mmol L^{-1} U of the matrix (Figure 10). While each addition of electroactive species almost did not cause any increment in the current, the additions of glucose of 1.0 mmol L^{-1} a remarkable increase showed in the current. The results indicate that the proposed sensors have good selectivity for detection of glucose. These biosensors can be used in determination of glucose in the presence of such electroactive interfering species.

Reusability and Storage Stability of Pt/P*o*PD–CSA/GOx and Pt/P*o*PD–ClO_4/GOx Electrodes. To evaluate the reusability of biosensors, three calibration curves were successively plotted according to amperometric response to glucose concentration in linear range using the same enzyme electrode. The relative standard deviation of the slopes of the calibration curves of Pt/P*o*PD–CSA/GOx and Pt/P*o*PD–ClO_4/GOx electrodes were found to be 2.6 and 4.1%, respectively (Supporting Information Figure S3). This result shows that the reusability of the enzyme electrodes is extremely adequate and these electrodes can be used for many analyses.

The storage stability of the biosensors was examined by amperometric response to 1.0 mmol L^{-1} glucose in PBS (pH = 7.0, 0.15 mol L^{-1}). After each measurement, the biosensors was washed with PBS and stored in a refrigerator at 4°C. The

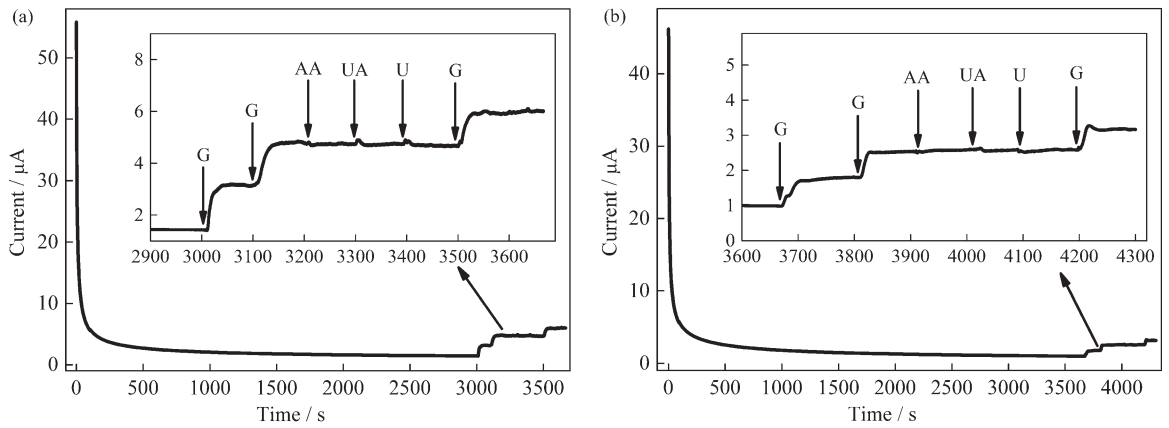

Figure 10. Effects of interfering AA, UA, and U on the amperometric response of the (a) Pt/P*o*PD–CSA/GOx and (b) Pt/P*o*PD–ClO_4/GOx electrodes to glucose at +0.7 V versus Ag/AgCl (0.15 mol L^{-1} PBS, pH 7.0).

Pt/PoPD–CSA/GOx electrode presented no remarkable decrease in current response in the first 3 weeks. The electrode was able to continue about 95% and 48% of the initial current response after 3 weeks and 1 month of storage, respectively. The Pt/PoPD–ClO_4/GOx electrode retained 66% and 50% of its initial current response to glucose after 5 and 10 days, respectively. The Pt/PoPD–CSA/GOx electrode exhibited higher long-term stability than the Pt/PoPD–ClO_4/GOx electrode. This result can possibly be contributed to the covalent bonding and interaction of the PoPD–CSA film and GOx is stronger than that of PoPD–ClO_4 film. The covalent bonding of GOx on the Pt/PoPD–CSA electrode avoids its leaching from the electrode surface to solution during process and storage.[52]

CONCLUSIONS

The electrochemical synthesis of PoPD film was performed for the first time in acetonitrile–water medium containing *o*PD monomer and HCSA on Pt electrode by using cyclic voltammetry method. The enzyme electrode that was prepared by immobilizing GOx enzyme using glutaraldehyde upon the PoPD–CSA coated electrode was examined to determine the glucose. The performance properties of this electrode were compared to those of Pt/PoPD–ClO_4 coated electrode that was prepared in the presence of $HClO_4$. The Pt/PoPD–CSA/GOx enzyme electrode possesses a higher affinity and sensitivity to glucose than that of Pt/PoPD–ClO_4/GOx electrode due to the CSA^- ion as dopant. This electrode with low detection limit can be applied in a very wide linear range to determine of glucose. Furthermore, the sensor can be used in many analyses due to having highly reusability and nearly interference-free. Consequently, the performance characteristics of these electrodes can compete with those of other electrodes previously reported in the literature.

ACKNOWLEDGMENTS

The authors thank the Scientific and Technological Research Council of Turkish (Project No: 106T359) and the Ankara University Scientist Training Project (Project No: 2005K120140-7) for their financial support.

REFERENCES

1. Chaubey, A.; Malhotra, B. D. *Biosensors Bioelectron.* **2002**, *17*, 441.
2. Montornes, J. M.; Vreeke, M. S.; Katakis, I. in Bioelectrochemistry: Fundamentals, Experimental Techniques and Applications; Bartlett, P.N., Eds; Wiley: Chichester, **2008**, pp. 199–217.
3. Vidal, J. C.; García, E.; Castillo, J. R. *Sens. Actuators B: Chem.* **1999**, *57*, 219.
4. Yuqing, M.; Jianrong, C.; Xiaohua, W. *Trends Biotechnol.* **2004**, *22*, 227.
5. Malitesta, C.; Palmisano, F.; Torsi, L.; Zambonin, P. G. *Anal. Chem.* **1990**, *62*, 2735.
6. Sasso, S. V.; Pierce, R. J.; Walla, R.; Yacynych, A. M. *Anal. Chem.* **1990**, *62*, 1111.
7. Lowry, J. P.; McAteer, K.; El Atrash, S. S.; Duff, A.; O'Neill, R. D. *Anal. Chem.* **1994**, *66*, 1754.
8. Dumont, J.; Fortier, G. *Biotechnol. Bioeng.* **1996**, *49*, 544.
9. de Corcuera, J. I. R.; Cavalieri, R. P.; Powers, J. R. *J. Electroanal. Chem.* **2005**, *575*, 229.
10. Chiba, K.; Ohsaka, T.; Ohnuki, Y.; Oyama, N. *J. Electroanal. Chem.* **1987**, *219*, 117.
11. Yano, J. *J. Polym. Sci. Part A: Polym. Chem.* **1995**, *33*, 2435.
12. Sivakkumar, S. R.; Saraswathi, R. *J. Appl. Electrochem.* **2004**, *34*, 1147.
13. Martinusz, K.; Czirók, E.; Inzelt, G. *J. Electroanal. Chem.* **1994**, *379*, 437.
14. Mazeikiene, R.; Malinauskas, A. *Synth. Met.* **2002**, *128*, 121.
15. Ogura, K.; Kokura, M.; Yano, J.; Shiigi, H. *Electrochim. Acta* **1995**, *40*, 2707.
16. Sánchez, C. O.; Rivas, B. L. *J. Appl. Polym. Sci.* **2002**, *85*, 2564.
17. Zhou, Q.; Zhuang, L.; Lu, J.; Li, C. M. *J. Phys. Chem. C* **2009**, *113*, 11346.
18. Angélica del Valle, M.; Díaz, F. R.; Bodini, M. E.; Alfonso, G.; Soto, G. M.; Borrego, E. D. *Polym. Int.* **2005**, *54*, 526.
19. Wu, L.-L.; Luo, J.; Lin, Z.-H. *J. Electroanal. Chem.* **1996**, *417*, 53.
20. Ogura, K.; Shiigi, H.; Nakayama, M.; Fujii, A. *J. Electrochem. Soc.* **1998**, *145*, 3351.
21. Hermas, A. A.; Wu, Z. X.; Nakayama, M.; Ogura, K. *J. Electrochem. Soc.* **2006**, *153*, B199.
22. Razmi, H.; Habibi, E. *J. Solid State Electrochem.* **2009**, *13*, 1897.
23. D'Elia, L. F.; Ortiz, R. L.; Marquez, O. P.; Marquez, J.; Martinez, Y. *J. Electrochem. Soc.* **2001**, *148*, C297.
24. Barbero, C.; Silber, J. J.; Sereno, L. *J. Electroanal. Chem.* **1989**, *263*, 333.
25. Hao, Q.; Lei, W.; Xia, X.; Yan, Z.; Yang, X.; Lu, L.; Wang, X. *Electrochim. Acta* **2010**, *55*, 632.
26. Ayad, M. M.; Zaki, E. A. *Eur. Polym. J.* **2008**, *44*, 3741.
27. Xia, Y.; MacDiarmid, A. G.; Epstein, A. J. *Macromolecules* **1994**, *27*, 7212.
28. Riaz, U.; Ashraf, S. M. *Chem. Eng. J.* **2011**, *174*, 546.
29. Bouldin, R. M.; Kyriazidis, L.; Fidler, A.; Ravichandran, S.; Kumar, J.; Samuelson, L. A.; Nagarajan, R. *J. Macromol. Sci.: Pure Appl. Chem.* **2011**, *48*, 976.
30. Pekmez, N.; Pekmez, K.; Arca, M.; Yildiz, A. *J. Electroanal. Chem.* **1993**, *353*, 237.
31. Wallace, G. G.; Spinks, G. M.; Kane-Maguire, L. A. P.; Teasdale, P. R. Conductive Electroactive Polymers: Intelligent Polymer SystemsBaco Raton; 3rd Ed.; CRC Press: Baco Raton, **2008**, pp. 59–101.
32. Wei, Y.; Chan, C. C.; Tian, J.; Jang, G. W.; Hsueh, K. F. *Chem. Mater.* **1991**, *3*, 888.
33. Lin, X.; Zhang, H. *Electrochim. Acta* **1996**, *41*, 2019.
34. Lu, X.; Mao, H.; Chao, D.; Zhao, X.; Zhang, W.; Wei, Y. *Mater. Lett.* **2007**, *61*, 1400.
35. Du, Y.; Wang, H.; Zhang, A.; Lu, J. *Chin. Sci. Bull.* **2007**, *52*, 2174.

36. Baibarac, M.; Baltog, I.; Scocioreanu, M.; Ballesteros, B.; Mevellec, J. Y.; Lefrant, S. *Synth. Met.* **2011**, *161*, 2344.
37. Qu, L.; Shi, G.; Yuan, J.; Han, G.; Chen, F. E. *J. Electroanal. Chem.* **2004**, *561*, 149.
38. Li, X.-G.; Huang, M.-R.; Duan, W.; Yang, Y.-L. *Chem. Rev.* **2002**, *102*, 2925.
39. Umare, S. S.; Waware, U. S.; Ingole, S.; Viswanath, S. G. *Int. J. Polym. Anal. Charact.* **2005**, *10*, 1.
40. Levin, O.; Kondratiev, V.; Malev, V. *Russ. J. Electrochem.* **2008**, *44*, 98.
41. Salam, M. A.; Al-Juaid, S. S.; Qusti, A. H.; Hermas, A. A. *Synth. Met.* **2011**, *161*, 153.
42. Du, P.; Li, H.; Mei, Z.; Liu, S. *Bioelectrochemistry* **2009**, *75*, 37.
43. Selvaraju, T.; Ramaraj, R. *J. Appl. Electrochem.* **2003**, *33*, 759.
44. Liu, Z.; Huang, S.; Jiang, D.; Liu, B.; Kong, J. *Anal. Lett.* **2004**, *37*, 2283.
45. Wang, J. Analytical Electrochemistry; 3rd Ed.; Wiley: New Jersey, **2006**, pp. 29–66.
46. Forzani, E. S.; Zhang, H.; Nagahara, L. A.; Amlani, I.; Tsui, R.; Tao, N. *Nano Lett.* **2004**, *4*, 1785.
47. Rüdel, U.; Geschke, O.; Cammann, K. *Electroanalysis* **1996**, *8*, 1135.
48. Yao, T.; Takashima, K. *Biosensors Bioelectron.* **1998**, *13*, 67.
49. Dai, Y.-Q.; Shiu, K.-K. *Electroanalysis* **2004**, *16*, 1806.
50. Zhou, D.-M.; Dai, Y.-Q.; Shiu, K.-K. *J. Appl. Electrochem.* **2010**, *40*, 1997.
51. Wang, J. Analytical Electrochemistry; 3rd Ed.; Wiley: New Jersey, **2006**, pp. 201–243.
52. Wan, D.; Yuan, S.; Li, G. L.; Neoh, K. G.; Kang, E. T. *ACS Appl. Mater. Interf.* **2010**, *2*, 3083.
53. Çiftçi, H.; Tamer, U.; Teker, M. Ş.; Pekmez, N. Ö. *Electrochim. Acta* **2013**, *90*, 358.